Early Changes in Functional Dynamic Magnetic Resonance Imaging Predict for Pathologic Response to Neoadjuvant Chemotherapy in Primary Breast Cancer

Mei-Lin W. Ah-See,[1] Andreas Makris,[1] N. Jane Taylor,[1] Mark Harrison,[1] Paul I. Richman,[1] Russell J. Burcombe,[1] J. James Stirling,[1] James A. d'Arcy,[2] David J. Collins,[2] Michael R. Pittam,[3] Duraisamy Ravichandran,[3] and Anwar R. Padhani[1]

Abstract

Purpose: Dynamic contrast-enhanced magnetic resonance imaging (DCE-MRI) allows non-invasive, *in vivo* measurements of tissue microvessel perfusion and permeability. We examined whether DCE-MRI done after two cycles of neoadjuvant chemotherapy could predict final clinical and pathologic response in primary breast cancers.

Experimental Design: Thirty-seven patients with primary breast cancer, due to receive six cycles of neoadjuvant 5-fluorouracil, epirubicin and cyclophosphamide chemotherapy, were examined using DCE-MRI before neoadjuvant chemotherapy and after two cycles of treatment. Changes in DCE-MRI kinetic parameters (K^{trans}, k_{ep}, v_e, MaxGd, rBV, rBF, MTT) were correlated with the final clinical and pathologic response to neoadjuvant chemotherapy. Test-retest variability was used to determine individual patient response.

Results: Twenty-eight patients were evaluable for response (19 clinical responders and 9 non-responders; 11 pathologic responders and 17 nonresponders). Changes in the DCE-MRI kinetic parameters K^{trans}, k_{ep}, MaxGd, rBV, and rBF were significantly correlated with both final clinical and pathologic response ($P < 0.01$). Change in K^{trans} was the best predictor of pathologic nonresponse (area under the receiver operating characteristic curve, 0.93; sensitivity, 94%; specificity, 82%), correctly identifying 94% of nonresponders and 73% of responders. Change in MRI-derived tumor size did not predict for pathologic response.

Conclusion: Changes in breast tumor microvessel functionality as depicted by DCE-MRI early on after starting anthracycline-based neoadjuvant chemotherapy can predict final clinical and pathologic response. The ability to identify nonresponders early may allow the selection of patients who may benefit from a therapy change.

Neoadjuvant chemotherapy (also termed primary systemic therapy) is used in women with primary breast cancer with the aim of tumor downsizing and downstaging to increase the chances of breast-conserving surgery and for treating occult micrometastatic disease. Neoadjuvant chemotherapy gives high clinical response rates (70-98%) and can result in a pathologically complete response in a subgroup of patients (3-34%; refs. 1–4). A variable proportion (2-30%) of patients may not benefit clinically or pathologically, and the ability to identify these women early on would enable the use of alternative therapies that may be more effective (5).

Response to neoadjuvant chemotherapy is currently assessed using the combination of clinical examination and conventional imaging techniques, such as mammography and breast ultrasound. These methods, however, often fail to inform upon final pathologic response, which is the best predictor of long-term outcome (1). As a result, newer functional imaging techniques, such as positron emission tomography (6) and dynamic magnetic resonance imaging (MRI; ref. 7), are under evaluation to determine their ability to classify tumor response earlier on in treatment, and hence facilitate the tailoring of treatment to response.

Relaxivity-based dynamic contrast-enhanced MRI (DCE-MRI), also called T_1-weighted (T_1W) DCE-MRI has become established as the means of imaging breast tumor microcirculation (8, 9) and refers to increases in tissue signal intensity over time due to the presence of diluted, low-molecular weight contrast media in the extravascular, extracellular space. The T_1W DCE-MRI kinetic parameter, transfer constant, K^{trans}, describes the transendothelial transport of contrast medium by diffusion

Authors' Affiliations: [1]Academic Oncology Unit and Paul Strickland Scanner Centre, Mount Vernon Hospital, Northwood, Middlesex, United Kingdom; [2]CRC Clinical MR Research Group, Royal Marsden Hospital, Sutton, Surrey, United Kingdom; and [3]Breast Unit, Luton & Dunstable Hospital NHS Trust, Luton, United Kingdom

Received 9/13/07; revised 2/12/08; accepted 2/28/08.

Grant support: Breast Cancer Research Trust and Childwick Trust.

The costs of publication of this article were defrayed in part by the payment of page charges. This article must therefore be hereby marked *advertisement* in accordance with 18 U.S.C. Section 1734 solely to indicate this fact.

Requests for reprints: Mei-Lin W. Ah-See, Academic Oncology Unit, Mount Vernon Hospital, Northwood, Middlesex HA6 2RN, United Kingdom. Phone: 44-1923-844805; Fax: 44-1923-844167; E-mail: meilinahsee@hotmail.com.

doi:10.1158/1078-0432.CCR-07-4310

from the vascular space to the tumor interstitium and provides a measure of vascular permeability and blood flow in breast tumors (10). In untreated breast tumors, K^{trans} is dominated by perfusion because of high first pass extraction related to microvessel immaturity. This has been determined in simulations and by empirical observations in xenografts and in human tumors (11, 12). This situation changes once vascular shutdown begins to occur with successful therapy when vascular permeability dominates K^{trans}. Another technique called dynamic susceptibility contrast MRI, or T_2*-weighted (T_2*W) DCE-MRI, assesses tissue signal intensity decreases with time due to the presence of concentrated contrast media within the vascular space. Here, the contrast medium acts as an intravascular tracer during the first passage through the circulatory system, and measurements of the relative blood flow (rBF) and relative blood volume (rBV) within a tumor can be obtained. A small number of DCE-MRI studies have evaluated breast tumor response to neoadjuvant chemotherapy, but none that have used first pass susceptibility techniques (7, 13, 14). Thus, we conducted a prospective study to evaluate the nature of the T_1W and T_2*W DCE-MRI–derived angiogenic response observed in women receiving neoadjuvant chemotherapy for primary breast cancer and to determine whether the DCE-MRI changes, when measured early on in treatment, could predict for the final clinical and pathologic response on a group and an individual patient basis.

Patients and Methods

Patients and treatment. Local ethics committee approval for the trial protocol and written informed consent from all participating patients were obtained. Between October 2001 and June 2003, 37 patients with primary breast cancer were enrolled into the study.

Women with newly diagnosed, nonmetastatic, histologically proven, locally advanced breast cancer who were due to receive six cycles of neoadjuvant FEC (5-fluorouracil 600mg/m^2 i.v., epirubicin 60mg/m^2 i.v., and cyclophosphamide 600mg/m^2 i.v. q21) chemotherapy were eligible for the study. This chemotherapy regimen was the standard neoadjuvant schedule in our institution at the time of the study. Taxanes were not routinely used. Additional inclusion criteria were (*a*) age 18-70 y old, (*b*) WHO performance status 0 or 1 (15), (*c*) not lactating or pregnant, (*d*) no contraindications to FEC chemotherapy, and (*e*) absolute neutrophil count >1.5 $\times$ 10^9/L and platelets >100 $\times$ 10^9/L. The exclusion criteria were (*a*) MRI scan contraindicated and (*b*) known allergy to gadopentetate dimeglumine (Gd-DTPA). Pretreatment assessments included full clinical history and physical examination, hematologic and biochemical blood screen, bilateral mammography, breast ultrasound, and core biopsy +/- fine needle aspiration cytology of the primary breast tumor.

Study design. Patients had DCE-MRI studies before the initiation of chemotherapy and 6 wk later after two cycles of therapy. Patients were assessed clinically before each cycle of chemotherapy and continued to a total of six cycles provided that there was no clinical evidence of progressive disease. At completion of chemotherapy, patients were reassessed clinically and radiologically (mammography +/- ultrasound) and further treatment (surgery, radiotherapy, and tamoxifen) recommended according to the response to chemotherapy, the clinician's discretion, and patient choice.

Of the 37 patients enrolled, 9 were not evaluable due to the following reasons: failure to tolerate the first MRI scan (n = 4), failure to fit into the scanner (n = 1), failure to undergo the second scan (n = 2), and the second MRI scan done following three cycles of chemotherapy due to patient factors (n = 2). Thus, there were 28 evaluable patients with a median age of 46 y (range, 29-70 y). The median number of cycles of neoadjuvant FEC chemotherapy received was 6 (range, 2-7 cycles). Seventeen patients were premenopausal and 11 were postmenopausal. The median time between scans was 42 d (range, 34-49 d) and the median time from first DCE-MRI scan to the first cycle of FEC chemotherapy was 2 d (range, 0-10 d). Details of the clinical stage of disease at diagnosis, tumor pathology, treatment administered, and response to treatment (clinical and pathologic) are shown in Table 1.

A reproducibility cohort of 12 patients was also studied to assess test-retest variability. These patients were examined by DCE-MRI twice within 1 wk before commencing therapy (either neoadjuvant chemotherapy or primary surgery). The reproducibility cohort patient characteristics were similar to the treatment cohort.

Dynamic MRI protocol. All patients were examined on a 1.5T Siemens Symphony scanner (Siemens Medical Systems) using a dedicated breast coil. Initial T_1W and T_2*W anatomic scans were done to select a sagittal imaging plane through the center of the tumor. Proton density–weighted gradient recall echo images were acquired first (TR 350 ms, TE 4.7 ms, flip angle 6°, slice thickness 8 mm) for 4 slices (3 through the tumor and 1 through the contralateral normal breast). Dynamic T_1W images were then acquired at a time resolution of 12 s per measurement for 40 measurements (TR 11 ms, TE 4.7 ms, flip angle 35°, total imaging time 8 min 5 s) at the same slice positions as the proton density images. Gd-DTPA (Schering Health Care Ltd.) was injected i.v. using a power injector [dose 0.1 mmol/kg body weight (bw)] at 4 mL/s during the fifth acquisition. Following this, a T_2*W DCE-MRI sequence was used to acquire data every 2 s over 2 min (TE 20ms, TR 30ms, flip angle = 40°, 1 slice through the center of the tumor) with 0.2 mmol/kg bw Gd-DTPA at 4 mL/s after 20 s. The entire anatomic and functional imaging protocol took between 40 and 50 min to complete.

The architectural features of the breast on precontrast anatomic images were used to guide the placement of scan planes. The reproducibility of this procedure was assured as far as possible, making sure that the same technologist performed the procedure, with the final chosen positions determined by a consensus opinion of the technologist, the attending physicist, and the research fellow. In cases of doubt, the supervising radiologist made the final decision. When there was a significant change after therapy in responders, then the slice planes were adapted to the new morphology. Uncertainties introduced by these determinations were taken into account by gauging responses in relation to the reproducibility statistic (see below) that takes into account patient set-up errors, machine measurement variability, and intrinsic tumor fluctuations of blood flow and permeability.

MRI image analysis. The MRI-defined tumor size [product of the maximal bidimensional measurements on the early post-contrast subtraction enhanced image (120 s)] was also determined at each scan and the change in size following two cycles of neoadjuvant chemotherapy was calculated.

All calculations were done pixel-by-pixel using custom analysis software called MRI Workbench (MRIW) that was developed at the Institute of Cancer Research, Royal Marsden Hospital, London, United Kingdom (16). Using information from anatomic and post-contrast T_1W DCE-MRI subtraction images, irregular regions of interest were carefully drawn around the tumor edges on all slices by a radiologist (ARP) with eight years of experience in DCE-MRI, who carefully excluded areas of artifact and blood vessels. Whole tumor regions of interest were placed to enable evaluation of the whole tumor response to therapy. Unlike most breast cancer studies where only the most enhancing area is evaluated, usually for diagnostic purposes, whole tumor regions of interest evaluation has been endorsed by an international consensus panel on DCE-MRI methodology for use in clinical trials (17), and has been the methodology used in other DCE-MRI response assessment trials such as those evaluating antiangiogenic therapies. Regions of interest were placed at similar locations on

pretreatment and posttreatment examinations, as far as was possible, taking into account changes in tumor size.

Signal intensity values on the T_1W images were converted to Gd-DTPA concentrations and subsequently Gd-DTPA concentration-time curves were fitted on a pixel-by-pixel basis to the Tofts and Kermode bidirectional kinetic model (18) using methods previously described (19) using a group plasma curve as described by Weinmann (20). The quantitative T_1W kinetic parameters, transfer constant (K^{trans}; units: min^{-1}), leakage space (v_e; units: %), rate constant (k_{ep}; units: min^{-1}), and maximum Gd-DTPA concentration (MaxGd; units: mmol/kg) were calculated using data from all image slices passing through the tumor. The quantitative T_2*W kinetic parameters, relative blood volume (rBV; units: arbitrary units), relative blood flow (rBF; units: arbitrary units), and mean transit time (MTT; units: sec) were calculated pixel-by-pixel using the Central Volume Theorem (BF = BV/MTT). The MTT refers to the time in seconds that it takes for the contrast medium to pass through tissues.

Pixels from the whole tumor regions of interest from all slices (3 slices on T_1W DCE-MRI and central tumor slice from T_2*W DCE-MRI) were combined, and the median value for each parameter was calculated from the resulting histogram data for the pretreatment and following two cycles of FEC chemotherapy DCE-MRI scans, and the treatment changes calculated.

Evaluation of tumor response to neoadjuvant chemotherapy. Clinical response was evaluated by clinical examination from the bidimensional measurements of the primary breast tumor before and following six cycles of FEC chemotherapy and was defined in accordance with the International Union Against Cancer criteria (21). For the study analysis, clinical responders were defined as those patients with complete response (cCR) or partial response (cPR). Clinical nonresponders were defined as those patients with stable disease (cSD) or progressive disease (cPD).

Pathologic response was evaluated by a comparison of the pretreatment core biopsy and the postchemotherapy surgical resected specimen. Response was graded 1 to 5 in accordance with previously described criteria (22–24) by a consultant pathologist (PIR). The pathologic grade definitions and illustrative examples are shown in Fig. 1. For the study analysis, pathologic responders were defined as those patients with grade 1, 2, 3, or 4 responses. Pathologic nonresponders were defined as those patients with a grade 5 response. This classification was used because although complete pathologic response (pCR) has been shown to predict for improved overall survival (25–27), its clinical usefulness is limited by the small number of patients (5-10%) who achieve such a response following anthracycline-based neoadjuvant chemotherapy. A system that groups patients with a complete or partial pathologic response together may be clinically more relevant especially as patients with a partial pathologic response can benefit clinically in terms of being able to undergo breast conservation. Further, despite the presence of macroscopic residual tumor following neoadjuvant chemotherapy (grade 4), the presence of chemotherapy-induced response features and a reduction in the tumor cell to stromal ratio has been shown to predict for an improved outcome in terms of both disease-free and overall survival at 5 y when compared with residual macroscopic disease in the absence of any response features (24).

Statistical analysis. Statistical analysis was done using the StatsDirect statistical software package (StatsDirect). Pretreatment parameter values and treatment changes were assessed in relation to clinical and

Table 1. MRI study population

Age, y	Menopausal status	TNM stage	Tumor grade and type	No. FEC cycles	Clinical response to FEC	Pathologic response (grade)
43	Pre	$T_2N_1M_0$	G3 IDC	6	PR	R (3)
56	Post	$T_2N_1M_0$	G2 IDC	6	CR	R (3)
34	Pre	$T_3N_0M_0$	G3 IDC	6	PR	R (4)
34	Pre	T_3N2M_0	G3 IDC	6	SD	NR (5)
46	Post	$T_{4d}N_1M_0$	NOS	5 (changed to docetaxel)	SD	NR*
38	Pre	$T_2N_0M_0$	G2 IDC	6	PR	R (4)
33	Pre	T_2N1M_0	G2 IDC	6	PR	NR (5)
45	Pre	$T_{4d}N_{3c}M_0$	IDC	6	CR	R (3 on bx)
59	Post	$T_2N_0M_0$	G2 IDC	6	PR	NR (5)
47	Pre	$T_2N_0M_0$	G2 IDC	6	CR	R (3)
51	Post	$T_3N_0M_0$	G3 IDC	6	PR	NR (5)
41	Pre	$T_{4d}N_1M_1$	NOS	7 (changed to paclitaxel/ trastuzumab)	PD	NR*
43	Pre	$T_{4a}N_0M_0$	IDC	4 (proceeded to surgery)	PD	NR (5)
39	Pre	$T_2N_1M_0$	IDC	6	SD	NR (5)
39	Pre	$T_2N_0M_0$	G2 IDC	6	PR	NR (5)
51	Post	$T_2N_{3c}M_0$	Mucinous	6	SD	NR (5)
29	Pre	$T_2N_1M_0$	G2 IDC	2 (proceeded to surgery)	PD	NR (5)
53	Pre	$T_3N_0M_0$	G2 lobular	6	PR	NR (5)
46	Pre	$T_2N_0M_0$	G2 IDC	6	PR	NR (5)
50	Post	$T_2N_0M_0$	G3 IDC	6	CR	R*
52	Post	$T_3N_0M_0$	G3IDC	6	CR	R*
53	Post	$T2N_0M_0$	G2 IDC	5 (due to side effects)	PR	R (4)
40	Pre	$T_3N_1M_0$	G2 IDC	6	PR	R (2)
70	Post	$T_{4b}N_0M_0$	G2 lobular	4 (proceeded to surgery)	PD	NR (5)
60	Post	$T_{4d}N_0M_0$	G3 IDC	6	PR	NR (5)
56	Post	$T_{4d}N_1M_0$	G1 lobular	6	SD	NR (5)
43	Pre	T_2N0M_0	G2 NOS	6	PR	NR (5)
47	Pre	$T_3N_0M_0$	G3 IDC	6	CR	R (3)

Abbreviations: IDC, invasive ductal carcinoma; NOS, breast cancer, not otherwise specified; bx, biopsy; R, with response; NR, no response.
*Patient did not receive surgery.

pathologic response following completion of chemotherapy using the Mann-Whitney *U* test (MW). Receiver operating characteristic curve analysis was used to determine which parameters best predicted for pathologic nonresponse. Area under the receiver operating characteristic curve, sensitivity, and specificity for each parameter were calculated. A P value of <0.05 was taken to represent statistical significance.

The statistical methods to determine test-retest variability (reproducibility) have been described previously (28–31). The 95% confidence interval is the key statistical parameter that is used to determine whether a change in a kinetic parameter following treatment is statistically significant. For each patient in the reproducibility cohort, the difference (d) between the two pretreatment measurements of a parameter was calculated. The square root of the mean squared difference, dsd ($= \sqrt{[(\Sigma d\ 2)/n]}$ where n is the number of patients), was then calculated. The 95% confidence interval for change for a group of n patients is then equal to $\pm(1.96 \times \text{dsd}/\sqrt{n})$. For an individual patient, $n = 1$, the 95% confidence interval for change is equal to $\pm(1.96 \times \text{dsd})$. This is known as the repeatability statistic, r, and is expressed as a percentage of the group mean pretreatment value for each parameter. It provides a range within which the difference between pretreatment and posttreatment values would be expected to lie for 95% of observations, assuming that no difference exists between the pretreatment and the posttreatment values. Thus, following the application of the repeatability statistic to an individual patient's data, if the difference (d) falls outside this range then a significant change is deemed to have occurred.

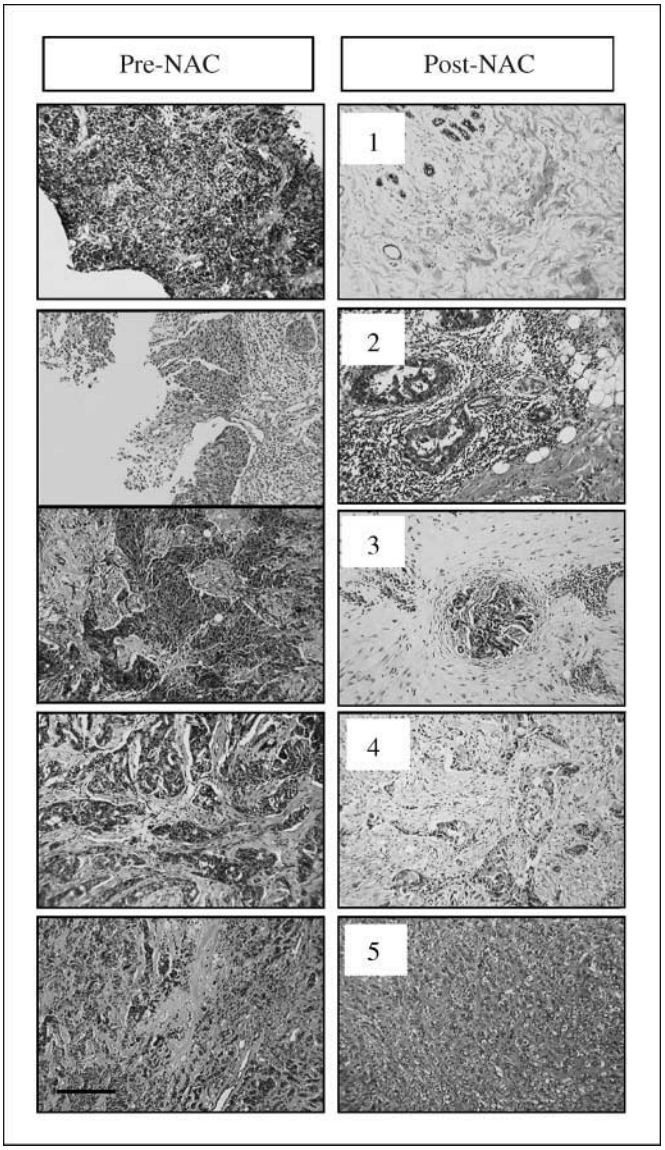

Fig. 1. Classification of the pathologic response grade and specimen examples. Examples of pretreatment primary breast cancer biopsy specimens are shown. Numbers refer to grade of pathologic response. Corresponding post-neoadjuvant chemotherapy (6 cycles) surgical specimen are shown; pathologic response grades are listed in Table 2. Scale bar, 250 μm.

Results

Response categorization. Two patients with a clinical and radiologic CR (as defined by mammography and breast ultrasound) who received radiotherapy alone were classified as pathologic responders. One patient obtained a clinical CR with a radiologic PR and received radiotherapy alone; a postchemotherapy biopsy of the residual radiologic abnormality showed a grade 3 pathologic response, and this patient was therefore classified as a pathologic responder also. Two patients with cSD and cPD, respectively, who received alternative chemotherapy without surgery were classified as pathologic nonresponders. This was deemed appropriate as 7 other patients classified as either cSD or cPD who did proceed to surgery were all scored as grade 5 pathologic nonresponders.

Thus, there were 19 clinical responders and 9 clinical nonresponders, giving an overall clinical response rate of 68%. There were 11 pathologic responders and 17 pathologic nonresponders, giving an overall pathologic response rate of 39%. Twenty-two patients completed all six cycles of FEC chemotherapy and proceeded to surgery; of these, only one patient achieved a pathologic CR, giving a pCR rate of 4.5%.

Pretreatment parameter data. There was no significant difference in the median pretreatment parameter values between primary breast tumors that showed an overall clinical or pathologic response after chemotherapy and those that did not (MW, $P > 0.05$ for all groups).

Parameter changes according to tumor response. Change in median K^{trans}, k_{ep}, MaxGd, rBV, and rBF significantly correlated with clinical response to neoadjuvant chemotherapy (MW, $P < 0.05$ for all groups). In responding tumors, there was a reduction in the median kinetic parameter values (K^{trans}, -39.8%; k_{ep}, -33.3%; MaxGd, -0.8%; rBV, -59.3%; rBF, -56.4%) and in the nonresponding tumors an increase in the median kinetic parameter values (K^{trans}, 18.1%; k_{ep}, 7.4%; MaxGd, 8.3%; rBV, 73.4%; rBF, 70.6%; Fig. 2).

Change in median K^{trans}, k_{ep}, MaxGd, rBV, and rBF were also significantly correlated with final pathologic response to neoadjuvant chemotherapy (MW, $P < 0.01$ for all groups). In those tumors that showed a pathologic response, there was a reduction in the median kinetic parameter values (K^{trans}, -52.3%; k_{ep}, -50.3%; MaxGad, -13.0%; rBV, -61.1%; rBF, -63.4%). This compared with a minor reduction or an increase in the median kinetic parameter values in the pathologically nonresponding tumors (K^{trans}, 16.9%; k_{ep}, -8.5%; MaxGd, 6.3%; rBV, -2.4%; and rBF, -3.5%; Fig. 2). Representative DCE-MRI anatomic and parametric images for a responding and a nonresponding patient are shown in Fig. 3.

Assessment of the change in MRI-derived tumor size following two cycles of neoadjuvant chemotherapy showed a reduction in tumor size in all response groups. In clinically responding tumors, there was a median reduction of 32.8% compared with 13.0% in the clinically nonresponding tumors, which was significantly different (MW, $P < 0.05$). In the tumors that showed pathologic response, there was a median reduction in MRI-derived tumor size of 35.5% compared with 14.8% in pathologic nonresponders. This difference was not statistically significant (MW, $P = 0.11$; Fig. 2). None of the size reductions seen following two cycles of neoadjuvant chemotherapy amounted to a partial response according to International Union Against Cancer criteria.

Receiver operating characteristic curve analysis was used to determine which parameter best predicted for pathologic nonresponse. This showed change in median K^{trans} to be the best predictor with an area under the receiver operating characteristic curve of 0.93 (sensitivity 94%, specificity 80%). Receiver operating characteristic analysis of size change following two cycles of neoadjuvant chemotherapy showed an area under the receiver operating characteristic curve of 0.68 (sensitivity 71%, specificity 73%).

The repeatability range was calculated for each parameter to predict pathologic nonresponse on an individual patient basis (Table 3). Application of the lower repeatability value to the DCE-MRI data revealed that change in K^{trans} predicted pathologic response most correctly, predicting nonresponse in 16 of 17 patients (94%) and pathologic response in 8 of 11 patients (73%; Fig. 4). This was superior to change in MRI-derived tumor size following application of the repeatability data, which was only able to correctly predict pathologic nonresponse in 10 of 17 patients (59%).

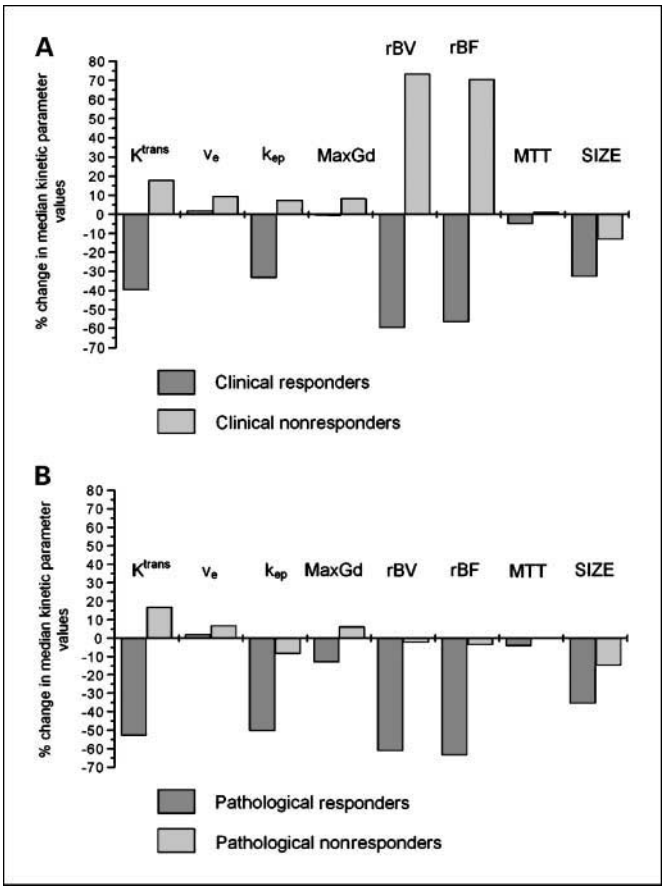

Fig. 2. Change in MRI-derived tumor size and DCE-MRI kinetic parameters according to (*A*) clinical tumor response and (*B*) pathologic tumor response. K^{trans}, transfer constant; v_e, leakage space; k_{ep}, rate constant; MaxGd, maximum Gd-DTPA concentration; rBV, relative blood volume; rBF, relative blood flow; MTT, mean transit time.

Discussion

Neoadjuvant chemotherapy in primary breast cancer is aimed at downsizing the primary tumor and treating potential micrometastatic disease. Clinical and pathologic primary tumor response to neoadjuvant chemotherapy represent intermediate surrogates of long-term outcome in primary breast cancer (27, 32, 33). An accurate assessment of tumor chemoresponsiveness early on during treatment might enable tailoring of therapy to the individual patient with the aim of increasing tumor response, which might translate into improved patient outcomes.

This is the first study to have examined in detail the ability of both T_1W and T_2*W DCE-MRI to act as early predictors of response to neoadjuvant chemotherapy. We found that changes in the quantitative parameters K^{trans}, k_{ep}, MaxGd, rBV, and rBF all correlated with both final clinical ($P < 0.05$) and pathologic response to neoadjuvant chemotherapy ($P < 0.01$), whereas change in MRI-derived tumor size following two cycles of neoadjuvant chemotherapy failed to correlate with final pathologic response. Furthermore, change in the T_1W parameter, K^{trans}, was the best predictor of pathologic nonresponse both at a group and an individual patient level. Thus, we have shown that patients who are destined to fail to respond to neoadjuvant chemotherapy can be reliably identified after just two cycles of therapy using DCE-MRI kinetic parameters that reflect on tumor blood flow and vascular permeability.

Traditionally, clinical examination and conventional imaging techniques, such as mammography and breast ultrasound, have been used to assess tumor size and response to treatment. Many studies have shown, however, that clinical examination, X-ray mammography, and ultrasonography are imperfect techniques for assessing tumor size and response to neoadjuvant chemotherapy as they are capable of both overestimating and underestimating the histologically defined tumor size (34–38). MRI has been shown to be superior to both mammography and ultrasonography in both the initial staging of primary breast cancer (39–42) and in the assessment of residual disease at the end of treatment (41, 43–45).

The value of functional DCE-MRI as an early predictor of the efficacy of neoadjuvant chemotherapy in primary breast cancer using both T_1W and T_2*W has not previously been fully assessed. It has been suggested that the morphologic MRI appearances of breast cancer before therapy can predict likelihood of response (46). A number of previous DCE-MRI studies done after successive cycles of therapy have shown that "successful" treatment can cause decreases in semiquantitative T_1W parameters, namely rate and magnitude of enhancement (an effect that becomes pronounced after two cycles), whereas a poor response results in persistent abnormal enhancement (13, 14). Both Padhani et al. and Martincich et al. also showed

that, whereas reductions in the early enhancement ratio after two cycles of neoadjuvant chemotherapy were associated with "major histological responses to treatment," reductions in tumor size/volume were equivalent predictors of pathologic response (7, 47). This is in contrast to our study results, where the change in DCE-MRI kinetic parameter values following two cycles of neoadjuvant chemotherapy (K^{trans}, k_{ep}, MaxGd, rBV, and rBF) was superior to change in MRI-derived tumor size for predicting pathologic response. It is well recognized that size change is an imperfect assessment method for assessing the effects of neoadjuvant chemotherapy. We found an appreciable discordance between final clinical and final pathologic response in our patient group, with almost a third of clinical responders (8 of 28) failing to obtain a pathologic response. This discrepancy between clinical and pathologic response has been described by others. The NSABP-B18 trial (27) showed that of the 682 patients who received neoadjuvant chemotherapy, 247 achieved a cCR but only 88 of these had a pCR. The European Organization for Research and Treatment of Cancer 10902 trial (26) showed similar results with 6 of 23 cCR patients experiencing a pCR. In addition, a further 7 patients achieved a pCR without a cCR. Thus, although others have shown that clinical response can be a useful predictor of pathologic response (33, 48), tumor shrinkage should be viewed as a crude measure of tumor response that is dependant on several variables including primary tumor size, edema, necrosis, and subjective variation in tumor measurement methods.

The pathologic nonresponse rate of 61% in our series is higher than that seen in the series from Ogston et al. (39% with Miller/Payne grade 1 or 2; ref. 24) and Chollet et al. (46% with Chevallier Class 4; ref. 49). Pathologic response in our study was evaluated by a single consultant pathologist (PIR) from a comparison of the pretreatment core biopsy and the postchemotherapy surgical resected specimen. A grading system for pathologic response was derived in accordance with the Miller/Payne grading system (24) assessing changes in tumor to stromal cellular ratio but also

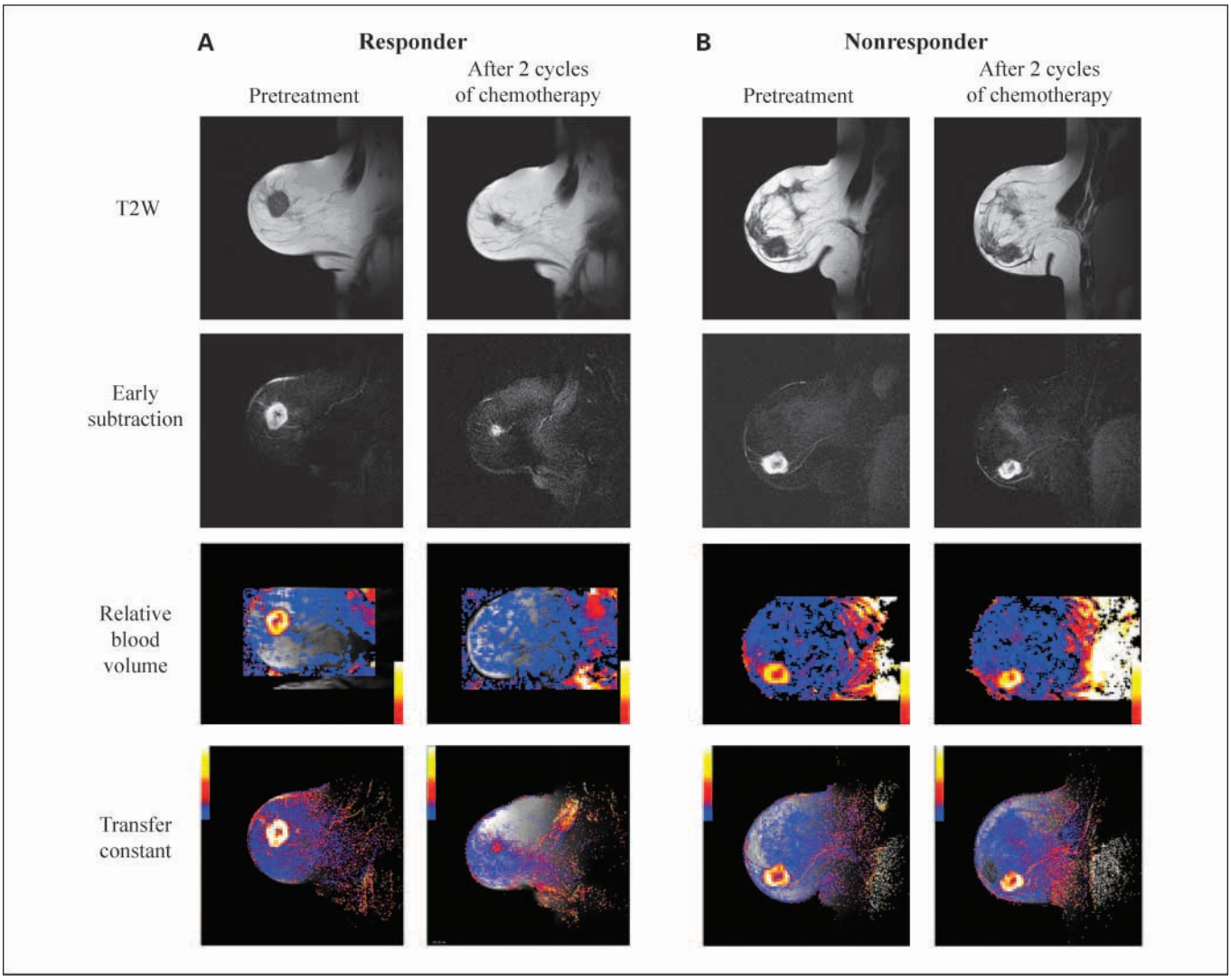

Fig. 3. Anatomic T_2W and T_1W early subtraction images and parametric maps for rBV and K^{trans} at baseline and following 2 cycles of neoadjuvant chemotherapy in a clinically and pathologically (*A*) responding patient and (*B*) nonresponding patient.

Table 2. Pathologic response

Pathologic response	Description
Grade 1	No residual invasive cancer or DCIS (pathologic CR)
Grade 2	Residual DCIS but no invasive cancer
Grade 3	Microscopic residual cancer
Grade 4	Macroscopic residual cancer with chemotherapy-induced changes* and/or histologic tumor response †
Grade 5	Macroscopic invasive cancer with no response features

*Enlarged cells; finely vacuolated "bubbly" voluminous cytoplasm; enlarged vesicular nucleus with prominent single eosinophilic nucleolus; occasionally enlarged hyperchromatic dense nucleus with an irregular outline; or compact hyalinized fibrous tissue at the site of good tumor response.
† Reduction in tumor cell to stroma ratio.

included other histologic features previously described elsewhere reflecting pathologic response to neoadjuvant chemotherapy (22, 23, 50). As yet, there is no single, universally employed scoring system for evaluating histologic response to neoadjuvant chemotherapy in breast cancer, with some overlap existing between the grades/classes of the different systems employed. The threshold for scoring a grade 4 pathologic response in our series was set high, and this may have accounted for the higher percentage of pathologic grade 5 nonresponding patients seen. Further consensus on how best to classify pathologic partial response to neoadjuvant chemotherapy is warranted.

The pathophysiologic basis for the DCE-MRI changes seen is not yet fully understood, but is likely to be multifactorial, relating to changes in both microvessel density and function due to antiangiogenic effects of the chemotherapy (51). Makris et al. reported that fewer tumor microvessels were seen in breast cancer patients treated with chemoendocrine therapy compared with untreated patients (52). However, they reported no differences in microvessel density counts between responders and nonresponders. It has been suggested that successful chemotherapy causes cytotoxic tumor cell death resulting in a reduction in tissue vascular endothelial growth factor levels and hence apoptosis of immature endothelial cells with secondary vascular shutdown (53). Indeed, in preliminary observations, we have shown a fall in the proportion of immature "proliferating" blood vessels in breast tumors following completion of neoadjuvant chemotherapy despite no associated change in the tumor microvessel density count (54). This decrease is associated with a reduction in the tumor vascular endothelial growth factor expression, which may result in preferential pruning of nonpericyte covered tumor microvessels. In contrast to our observations, however, the latter would in general cause reductions in microvessel density. The change in vessel maturity in the absence of changes in MVD is thus likely to be due to associated stromal compaction following neoadjuvant chemotherapy.

There are other limitations of our study, including the reproducibility of the MRI procedures given the pliable nature of the breast and because of tumor shrinkage with successful therapy. Uncertainties introduced can be partly taken into account by gauging responses in relation to the reproducibility statistic (see below) that takes into account patient set-up errors, machine measurement variability, and intrinsic tumor fluctuations of blood flow and permeability. Uncertainties do exist with regard to the reliability of kinetic parameter estimates derived from the application of tracer kinetic models

Table 3. Patient pathologic response as classified by DCE-MRI parameters and repeatability range for predicting response on an individual patient basis

Parameter	Repeatability range*	Correctly classified (patient nos.)	
		Nonresponders	Responders
K^{trans}	-42.4 to +73.6	94% (16/17)	73% (8/11)
v_e	-29.9 to +29.9	100% (17/17)	9% (1/11)
k_{ep}	-57.8 to +136.8	88% (15/17)	36% (4/11)
MaxGd	-18.8 to +18.8	100% (17/17)	36% (4/11)
rBV †	-74.9 to +74.9	88% (14/16)	20% (2/10)
rBF †	-63.9 to +63.9	88% (14/16)	20% (2/10)
MTT †	-22.1 to +22.1	88% (14/16)	0% (0/10)
Tumor size	-26.5 to +36.1	59% (10/17)	73% (8/11)

Abbreviations: K^{trans}, transfer constant; v_e, leakage space; k_{ep}, rate constant; MaxGd, maximum Gd-DTPA concentration; rBV, relative blood volume; rBF, relative blood flow; MTT, mean transit time.
*Repeatability range is the % change required for significance at 95% confidence for a single patient.
† T2W data only available on 26 patients.

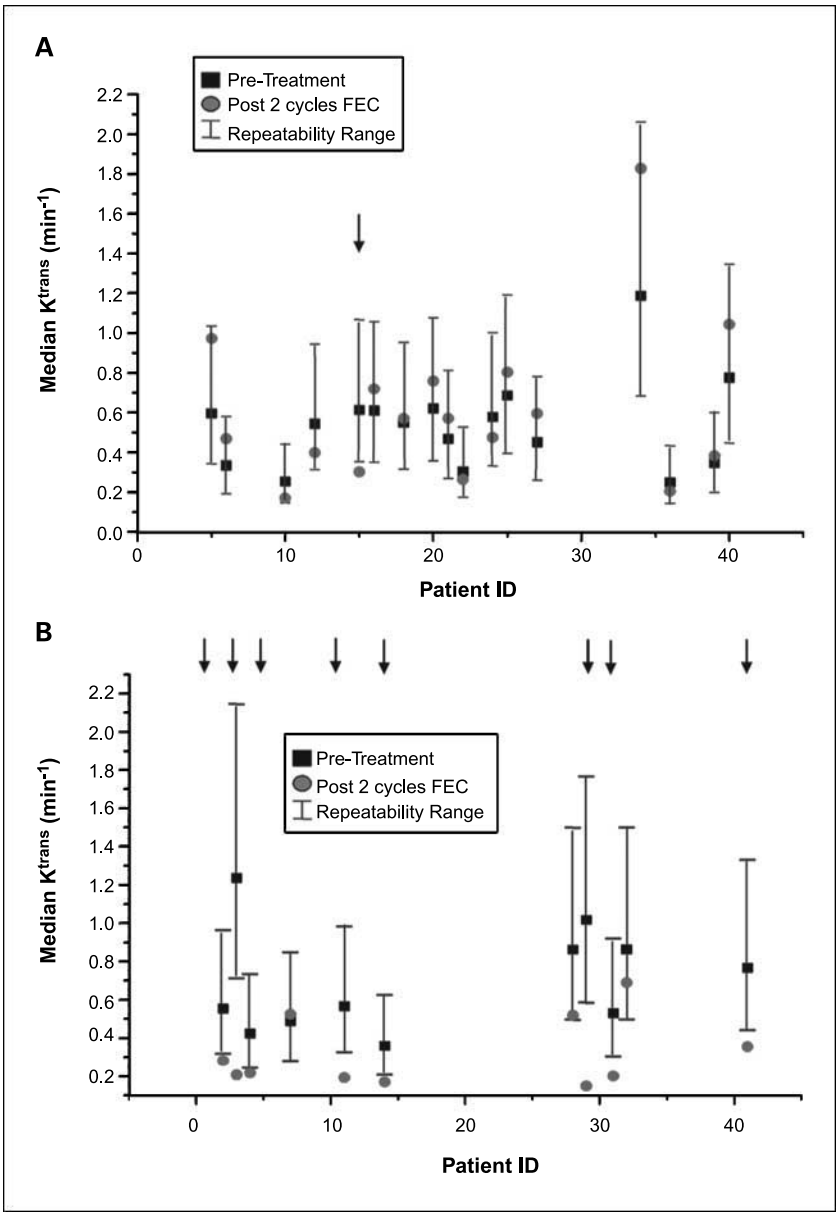

Fig. 4. K^{trans} repeatability range applied to (*A*) each pathologic nonresponding patient's data and showing no significant change in median K^{trans} in 16 of the 17 nonresponding patients (the arrow indicates the single incorrectly classified nonresponding patient), and (*B*) each pathologic responding patient's data and showing a significant reduction in median K^{trans} in 8 of the 11 responding patients (the arrows indicate these correctly classified responding patients).

to T_1- and T_2*-weighted DCE-MRI data. These derive from assumptions implicit in kinetic models and those for the measurement of tissue contrast agent concentration. For example, the Tofts' model uses a standard description of the time-varying blood concentration of the contrast agent, and assumes that the supply of contrast medium is not flow-limited and that tissue blood volume contributes negligibly to signal intensity changes compared with that arising from contrast medium in the interstitial space. We have used a 2-point technique (proton density and initial T_1-weighted image) to calculate relaxation values, but there are alternative schemes for calculating these values that may be more or equally accurate. The technique employed in this study, however, has been used successfully to assess vascular response to therapy. Furthermore, international consensus meetings have recognized that this is a controversial area and have sought not to be prescriptive in this regard (17), recognizing that despite these complexities, quantitative DCE-MRI kinetic parameters can provide insights into underlying tissue pathophysiologic processes and may provide a useful tool in treatment decision-making both in the clinic and in pharmaceutical drug development.

Thus, in this study we have done and established the intrinsic variability of kinetic parameters derived from susceptibility- (T_2*) and relaxivity(T_1W)-based dynamic MRI techniques in breast cancers and have shown the ability of DCE-MRI to accurately predict final pathologic response early on in therapy. The evaluation of patients using this technique before and following two cycles of anthracycline-based neoadjuvant chemotherapy for primary breast cancer would enable the identification of non-responding patients who may benefit from a therapy

change, and we now feel that there is sufficient confidence to proceed to multicenter clinical studies to assess the generalizability of this technique.

Disclosure of Potential Conflicts of Interest

No potential conflicts of interest were disclosed.

References

1. Rastogi P, Anderson SJ, Bear HD, et al. Preoperative chemotherapy: updates of National Surgical Adjuvant Breast and Bowel Project Protocols B-18 and B-27. J Clin Oncol 2008;26:778–85.
2. Bonadonna G, Valagussa P, Brambilla C, et al. Primary chemotherapy in operable breast cancer: eight-year experience at the Milan Cancer Institute. J Clin Oncol 1998;16:93–100.
3. Bear HD, Anderson S, Brown A, et al. The effect on tumor response of adding sequential preoperative docetaxel to preoperative doxorubicin and cyclophosphamide: preliminary results from National Surgical Adjuvant Breast and Bowel Project Protocol B-27. J Clin Oncol 2003;21:4165–74.
4. Makris A, Powles TJ, Ashley SE, et al. A reduction in the requirements for mastectomy in a randomized trial of neoadjuvant chemoendocrine therapy in primary breast cancer. Ann Oncol 1998; 9:1179–84.
5. Smith IC, Heys SD, Hutcheon AW, et al. Neoadjuvant chemotherapy in breast cancer: significantly enhanced response with docetaxel. J Clin Oncol 2002; 20:1456–66.
6. Smith IC, Welch AE, Hutcheon AW, et al. Positron emission tomography using [(18)F]-fluorodeoxy-D-glucose to predict the pathologic response of breast cancer to primary chemotherapy. J Clin Oncol 2000; 18:1676–88.
7. Martincich L, Montemurro F, De Rosa G, et al. Monitoring response to primary chemotherapy in breast cancer using dynamic contrast-enhanced magnetic resonance imaging. Breast Cancer Res Treat 2004; 83:67–76.
8. Jackson A. Analysis of dynamic contrast enhanced MRI. Br J Radiol 2004;:S154–66.
9. Padhani AR, Ah-See ML, Makris A. MRI in the detection and management of breast cancer. Expert Rev Anticancer Ther 2005;:239–52.
10. Tofts PS, Berkowitz B, Schnall MD. Quantitative analysis of dynamic Gd-DTPA enhancement in breast tumors using a permeability model. Magn Reson Med 1995;33:564–8.
11. Ferrier MC, Sarin H, Fung SH, et al. Validation of dynamic contrast-enhanced magnetic resonance imaging-derived vascular permeability measurements using quantitative autoradiography in the RG2 rat brain tumor model. Neoplasia 2007;9: 546–55.
12. Lankester KJ, Taylor JN, Stirling JJ, et al. Dynamic MRI for imaging tumor microvasculature: comparison of susceptibility and relaxivity techniques in pelvic tumors. J Magn Reson Imaging 2007;25: 796–805.
13. Knopp MV, Brix G, Junkermann HJ, Sinn HP. MR mammography with pharmacokinetic mapping for monitoring of breast cancer treatment during neoadjuvant therapy. Magn Reson Imaging Clin N Am 1994;2: 633–58.
14. Hayes C, Padhani AR, Leach MO. Assessing changes in tumour vascular function using dynamic contrast-enhanced magnetic resonance imaging. NMR Biomed 2002;15:154–63.
15. Oken MM, Creech RH, Tormey DC, et al. Toxicity and response criteria of the Eastern Cooperative Oncology Group. Am J Clin Oncol 1982;5:649–55.
16. D'Arcy J, Collins D, Padhani A, Walker-Samuel S, Suckling J, Leach M. Magnetic Resonance Imaging Workbench (MRIW): dynamic contrast enhanced MRI data analysis and visualisation. Radiographics 2006;26:621–32.
17. Leach MO, Brindle KM, Evelhoch JL, et al. The assessment of antiangiogenic and antivascular therapies in early-stage clinical trials using magnetic resonance imaging: issues and recommendations. Br J Cancer 2005;92:1599–610.
18. Tofts PS, Kermode AG. Measurement of the blood-brain barrier permeability and leakage space using dynamic MR imaging. 1. Fundamental concepts. Magn Reson Med 1991;17:357–67.
19. Galbraith SM, Lodge MA, Taylor NJ, et al. Reproducibility of dynamic contrast-enhanced MRI in human muscle and tumours: comparison of quantitative and semi-quantitative analysis. NMR Biomed 2002;15: 132–42.
20. Weinmann HJ, Laniado M, Mutzel W. Pharmacokinetics of GdDTPA/dimeglumine after intravenous injection into healthy volunteers. Physiol Chem Phys Med NMR 1984;167–72.
21. Hayward JL, Rubens RD, Carbone PP, Heuson JC, Kumaoka S, Segaloff A. Assessment of response to therapy in advanced breast cancer. A project of the programme on clinical oncology of the International Union against Cancer, Geneva, Switzerland. Eur J Cancer 1978;14:1291–2.
22. Sharkey FE, Addington SL, Fowler LJ, Page CP, Cruz AB. Effects of preoperative chemotherapy on the morphology of resectable breast carcinoma. Mod Pathol 1996;9:893–900.
23. Aktepe F, Kapucuoglu N, Pak I. The effects of chemotherapy on breast cancer tissue in locally advanced breast cancer. Histopathology 1996;29: 63–7.
24. Ogston KN, Miller ID, Payne S, et al. A new histological grading system to assess response of breast cancers to primary chemotherapy: prognostic significance and survival. Breast 2003;12:320–7.
25. Feldman LD, Hortobagyi GN, Buzdar AU, Ames FC, Blumenschein GR. Pathological assessment of response to induction chemotherapy in breast cancer. Cancer Res 1986;46:2578–81.
26. van der Hage JA, van de Velde CJ, Julien JP, Tubiana-Hulin M, Vandervelden C, Duchateau L. Preoperative chemotherapy in primary operable breast cancer: results from the European Organization for Research and Treatment of Cancer trial 10902. J Clin Oncol 2001;19:4224–37.
27. Wolmark N, Wang J, Mamounas E, Bryant J, Fisher B. Preoperative chemotherapy in patients with operable breast cancer: nine-year results from National Surgical Adjuvant Breast and Bowel Project B-18. J Natl Cancer Inst Monogr 2001;:96–102.
28. Bland J, Altman D. Measurement error proportional to the mean. BMJ 1996;313:106. Erratum in: BMJ 1996;313:744.
29. Bland J, Altman D. Measurement error [corrected and republished article originally printed in BMJ 1996 Jun 29; 312(7047):1654] [see comments]. BMJ 1996;313:744.
30. Galbraith S, Lodge M, Taylor N, et al. Reproducibility of dynamic contrast enhanced MRI in human muscle and tumours - comparison of quantitative and semi-quantitative analysis. NMR Biomed 2002; 15:132–42.
31. Padhani AR, Hayes C, Landau S, Leach MO. Reproducibility of quantitative dynamic MRI of normal human tissues. NMR Biomed 2002;15: 143–53.
32. Pierga JY, Mouret E, Laurence V, et al. Prognostic factors for survival after neoadjuvant chemotherapy in operable breast cancer. the role of clinical response. Eur J Cancer 2003;39:1089–96.
33. Cleator SJ, Makris A, Ashley SE, Lal R, Powles TJ. Good clinical response of breast cancers to neoadjuvant chemoendocrine therapy is associated with improved overall survival. Ann Oncol 2005;16: 267–72.
34. Herrada J, Iyer RB, Atkinson EN, Sneige N, Buzdar AU, Hortobagyi GN. Relative value of physical examination, mammography, and breast sonography in evaluating the size of the primary tumor and regional lymph node metastases in women receiving neoadjuvant chemotherapy for locally advanced breast carcinoma. Clin Cancer Res 1997;3:1565–9.
35. Allen SA, Cunliffe WJ, Gray J, et al. Pre-operative estimation of primary breast cancer size: a comparison of clinical assessment, mammography and ultrasound. Breast 2001;10:299–305.
36. Fiorentino C, Berruti A, Bottini A, et al. Accuracy of mammography and echography versus clinical palpation in the assessment of response to primary chemotherapy in breast cancer patients with operable disease. Breast Cancer Res Treat 2001;69: 143–51.
37. Pritt B, Ashikaga T, Oppenheimer RG, Weaver DL. Influence of breast cancer histology on the relationship between ultrasound and pathology tumor size measurements. Mod Pathol 2004.
38. Vinnicombe SJ, MacVicar AD, Guy RL, et al. Primary breast cancer: mammographic changes after neoadjuvant chemotherapy, with pathologic correlation. Radiology 1996;198:333–40.
39. Boetes C, Mus RD, Holland R, et al. Breast tumors: comparative accuracy of MR imaging relative to mammography and US for demonstrating extent. Radiology 1995;197:743–7.
40. Davis PL, Staiger MJ, Harris KB, et al. Breast cancer measurements with magnetic resonance imaging, ultrasonography, and mammography. Breast Cancer Res Treat 1996;37:1–9.
41. Esserman L, Hylton N, Yassa L, Barclay J, Frankel S, Sickles E. Utility of magnetic resonance imaging in the management of breast cancer: evidence for improved preoperative staging. J Clin Oncol 1999; 17:110–9.
42. Yang WT, Lam WW, Cheung H, Suen M, King WW, Metreweli C. Sonographic, magnetic resonance imaging, and mammographic assessments of preoperative size of breast cancer. J Ultrasound Med 1997;16: 791–7.
43. Gilles R, Guinebretiere JM, Toussaint C, et al. Locally advanced breast cancer: contrast-enhanced subtraction MR imaging of response to preoperative chemotherapy. Radiology 1994;191:633–8.
44. Weatherall PT, Evans GF, Metzger GJ, Saborrian MH, Leitch AM. MRI vs. histologic measurement of breast cancer following chemotherapy: comparison with x-ray mammography and palpation. J Magn Reson Imaging 2001;13:868–75.
45. Rieber A, Brambs HJ, Gabelmann A, Heilmann V, Kreienberg R, Kuhn T. Breast MRI for monitoring response of primary breast cancer to neo-adjuvant chemotherapy. Eur Radiol 2002;12:1711–9.
46. Esserman L, Kaplan E, Partridge S, et al. MRI phenotype is associated with response to doxorubicin and cyclophosphamide neoadjuvant chemotherapy in stage III breast cancer. Ann Surg Oncol 2001;8: 549–59.
47. Padhani AR, Hayes C, Assersohn L, et al. Prediction of clinicopathologic response of breast cancer to primary chemotherapy at contrast-enhanced MR imaging: initial clinical results. Radiology 2006;239: 361–74.

48. von Minckwitz G, Blohmer JU, Raab G, et al. *In vivo* chemosensitivity-adapted preoperative chemotherapy in patients with early-stage breast cancer: the GEPARTRIO pilot study. Ann Oncol 2005; 16:56–63.

49. Chollet P, Charrier S, Brain E, et al. Clinical and pathological response to primary chemotherapy in operable breast cancer. Eur J Cancer 1997;33: 862–6.

50. Chevallier B, Roche H, Olivier JP, Chollet P, Hurteloup P. Inflammatory breast cancer. Pilot study of intensive induction chemotherapy (FEC-HD) results in a high histologic response rate. Am J Clin Oncol 1993;16:223–8.

51. Kerbel RS, Klement G, Pritchard KI, Kamen B. Continuous low-dose anti-angiogenic/metronomic chemotherapy: from the research laboratory into the oncology clinic. Ann Oncol 2002;13: 12–5.

52. Makris A, Powles TJ, Kakolyris S, Dowsett M, Ashley SE, Harris AL. Reduction in angiogenesis after neoadjuvant chemoendocrine therapy in patients with operable breast carcinoma. Cancer 1999;85:1996–2000.

53. Darland DC, D'Amore PA. Blood vessel maturation: vascular development comes of age. J Clin Invest 1999;103:157–8.

54. Ah-See MW, Harris AL, Burcombe RJ, et al. Evaluation of the effect of neoadjuvant chemotherapy on tumour microvessel density (MVD), pericyte coverage index (PCI) & vascular endothelial growth factor (VEGF) in primary breast cancer [abstract]. Breast Cancer Res Treat 2005;94:S224.

Clinical Cancer Research

Early Changes in Functional Dynamic Magnetic Resonance Imaging Predict for Pathologic Response to Neoadjuvant Chemotherapy in Primary Breast Cancer

Mei-Lin W. Ah-See, Andreas Makris, N. Jane Taylor, et al.

Clin Cancer Res 2008;14:6580-6589.